Discrepancies between formaldehyde measurements and methane oxidation model predictions in the Antarctic troposphere: An assessment of other possible formaldehyde sources

K. Riedel and W. Allan
National Institute of Water and Atmospheric Research (NIWA), Wellington, New Zealand

R. Weller and O. Schrems
Alfred Wegener Institute for Polar and Marine Research, Bremerhaven, Germany

Received 8 February 2005; revised 11 May 2005; accepted 22 June 2005; published 13 August 2005.

[1] Formaldehyde (HCHO) is a key intermediate in the photooxidation of methane by hydroxyl radicals. Through its photolysis, it is also a source for free radicals in the troposphere. Owing to these reactions, HCHO influences the oxidation capacity of the atmosphere and is a suitable species to test our current understanding of atmospheric oxidation pathways. Especially in polar regions, discrepancies between measurements and model calculations exist. Though recent investigations in the Arctic suggest that HCHO emissions from the snow surface might act as the missing source, the question remains unresolved for the Antarctic. We compare year-round HCHO measurements in Antarctica with model results from a simple photochemical box model. The observed ambient HCHO mixing ratios cannot be explained by methane photooxidation alone. Inclusion of HCHO emissions from the snow surface makes the model results and measurements consistent, but significantly higher emissions than those derived in the Arctic are needed to explain the observed HCHO mixing ratios. We discuss and model other possible sources such as oxidation of dimethylsulfide (DMS), isoprene, ethene, propene, and the effect of halogens, that may be responsible for the enhanced HCHO mixing ratios in the marine Antarctic troposphere. We find that, for the largest HCHO mixing ratio measured, all potential gas-phase HCHO precursors (including methane) are likely to generate only 20–40% of the required HCHO. If the remaining HCHO is produced by a flux from the snow, the flux required is $1.9–2.5 \times 10^{13}$ molecules m^{-2} s^{-1} if the boundary layer height is 40–50 m.

Citation: Riedel, K., W. Allan, R. Weller, and O. Schrems (2005), Discrepancies between formaldehyde measurements and methane oxidation model predictions in the Antarctic troposphere: An assessment of other possible formaldehyde sources, *J. Geophys. Res.*, *110*, D15308, doi:10.1029/2005JD005859.

1. Introduction

[2] Formaldehyde (HCHO) is a key intermediate in the photooxidation of methane (CH_4) and many nonmethane hydrocarbons (NMHCs). In the clean troposphere, CH_4 is the most abundant hydrocarbon and under these conditions HCHO is thought to be mainly produced by the oxidation of CH_4 with hydroxyl radicals (OH) [*Lowe and Schmidt*, 1983].

[3] Sinks for HCHO are dry and wet deposition, reaction with OH radicals, and photolysis. The photolysis of HCHO yields either hydrogen atoms and HCO radicals or hydrogen molecules and carbon monoxide (CO) depending on the wavelength. With regard to these reactions, HCHO has to be considered (1) as a significant radical source and (2) as an important source for CO in the clean troposphere. Since photolytically produced hydrogen atoms can easily react with oxygen to form hydroperoxyl radicals (HO_2), HCHO is also a source of HO_2 in the upper troposphere where other sources of OH and ultimately HO_2 decrease in importance as the water vapor content decreases with altitude.

[4] Taking all these reactions into account, HCHO exerts an influence on the OH budget. Since the abundance of OH is often used as a metric for the oxidizing capacity of the atmosphere, HCHO must also influence this oxidizing capacity. Because of its involvement in many photochemical reactions, HCHO can be used to test our current understanding of photochemical hydrocarbon oxidation pathways. However, some recent studies have revealed big discrepancies between measurements and model calculations. In the marine boundary layer, models both over- and under-predict observations [*Fried et al.*, 2003a, and references therein]. Two studies found good agreement between observations and model results [*Fried et al.*, 2003a; *Wagner et al.*, 2002]. In the middle and upper troposphere, models

0148-0227/05/2005JD005859$09.00

generally tend to under-predict HCHO observations [*Fried et al.*, 2003a], suggesting either the presence of missing sources or faster removal processes not included in the models. *Ayers et al.* [1997] suggested that removal processes are probably of the right order of magnitude for HCHO. However, these studies were performed in mid-latitudes and did not consider snow processes. In this paper we will mainly concentrate on missing HCHO sources, but we will also touch on uncertainties in HCHO removal processes by deposition on snow surfaces.

[5] Several groups have found discrepancies between HCHO measurements and model calculations, and several attempts have been made to explain these discrepancies. A simplified set of reactions involving HCHO in a low NO_x environment is given by *Ayers et al.* [1997]. The following critical reactions and reaction summaries will be discussed in more detail.

$$(R1) \qquad NO_3^- + h\nu \rightarrow\rightarrow\rightarrow OH, O_3, O(^3P)$$

$$(R2) \qquad OH, O_3, O(^3P) + \text{dissolved organic material} \rightarrow\rightarrow\rightarrow HCHO$$

$$(R3) \qquad DMS + OH + O_2 + NO \rightarrow\rightarrow\rightarrow HCHO + CH_3S$$

$$(R4) \qquad CH_4 + Cl \rightarrow CH_3 + HCl$$

$$(R5) \qquad CH_3 + O_2 \rightarrow CH_3O_2$$

$$(R6) \qquad Br + HCHO \rightarrow HBr + CHO$$

$$(R7) \qquad BrO + HCHO \rightarrow HOBr + CHO$$

[6] In polar regions it was proved that the snow surface is a so far neglected source for HCHO. Investigations at Alert, Canada, and Summit, Greenland, have shown that a HCHO flux out of the snow can be measured [*Sumner and Shepson*, 1999; *Hutterli et al.*, 1999; *Jacobi et al.*, 2002; *Sumner et al.*, 2002; *Dassau et al.*, 2002]. Proposed sources for this HCHO were either outgassing from HCHO rich winter layers [*Hutterli et al.*, 1999], or photochemical reaction of organic matter in the snow with OH radicals produced by nitrate photolysis in the snow (reaction summaries (1) and (2), only precursors and some products shown) [*Sumner and Shepson*, 1999; *Honrath et al.*, 1999; *Dibb et al.*, 2002].

[7] Earlier studies had already considered NMHCs, which were not measured during the campaigns, as additional HCHO precursors [*Ayers et al.*, 1997; *Cox*, 1999; *Weller et al.*, 2000; *Lewis et al.*, 2001; *Fried et al.*, 2003b]. Terminal alkenes like ethene (C_2H_4), propene (C_3H_6), and isoprene (C_5H_8) are significantly more efficient in producing HCHO then alkanes on a per molecule basis [*Wert et al.*, 2003; *Lee et al.*, 1998].

[8] *Ayers et al.* [1997] discussed dimethylsulfide (DMS) as another possible HCHO precursor (reaction summary (3), only precursors and some products shown). Due to very low measured concentrations in the atmosphere [*Ayers et al.*, 1995], this idea was abandoned. However, recent measurements [*Curran and Jones*, 2000] show remarkably high DMS concentrations in ocean surface waters. Resulting estimates of DMS fluxes out of the ocean are large, up to 34.2×10^{13} molecules m^{-2} s^{-1} in January for the Southern Ocean. The main DMS flux can be expected when the sea-ice surrounding the Antarctic continent breaks up in spring and early summer.

[9] Another uncertainty in estimating the HCHO budget is the effect of halogen chemistry. Though CH_4 oxidation by OH is thought to be the main source for HCHO in the clean troposphere, oxidation by chlorine (Cl) is also possible (reactions (4) and (5)) [*Rudolph et al.*, 1999; *Platt*, 2002; *Sumner et al.*, 2002], and may generate a significant amount of HCHO in some regions when Cl concentrations are elevated.

[10] On the other hand, HCHO is also destroyed by Br and BrO (reactions (6) and (7)). During tropospheric ozone depletion events both Cl and Br atom concentrations are elevated. *Rudolph et al.* [1999] point out that ozone depletion episodes can be divided into two phases, one with partial ozone destruction when HCHO is increased due to the reaction of CH_4 with Cl, and the other with severe ozone destruction when HCHO is destroyed by reaction with Br and BrO. A decrease in HCHO mixing ratios when bromine concentrations exceed a certain limit was also observed by other groups [*Ridley et al.*, 2003; *Sumner and Shepson*, 1999].

[11] The purpose of this paper is to estimate the amount of HCHO needed in addition to the amount generated by normal gas-phase chemistry to match our observations with our model results. We will test if HCHO emissions out of the snow are effective enough to provide the necessary HCHO amounts, and we will further discuss whether precursors like DMS and isoprene are abundant enough in the Antarctic troposphere to give the elevated HCHO mixing ratios. The new approach of this paper is to include DMS and isoprene, not considered in any other study in polar regions, and to test if they can explain the elevated HCHO levels in combination with other precursors such as ethene and halogens. Our study shows that the contribution of these precursors is too small to have a significant influence on HCHO production. Instead, large HCHO fluxes from the snow surface appear to be required to account for the observed elevated HCHO mixing ratios at Neumayer.

2. Measurements and Model Description

2.1. Measurements

[12] The measurements were carried out at the German Antarctic station Neumayer (70°39′S, 08°15′W) (Figure 1) during the over–wintering season 1997/1998 and during a summer campaign from January to March 1999. Data from both measurement campaigns were combined in one seasonal cycle.

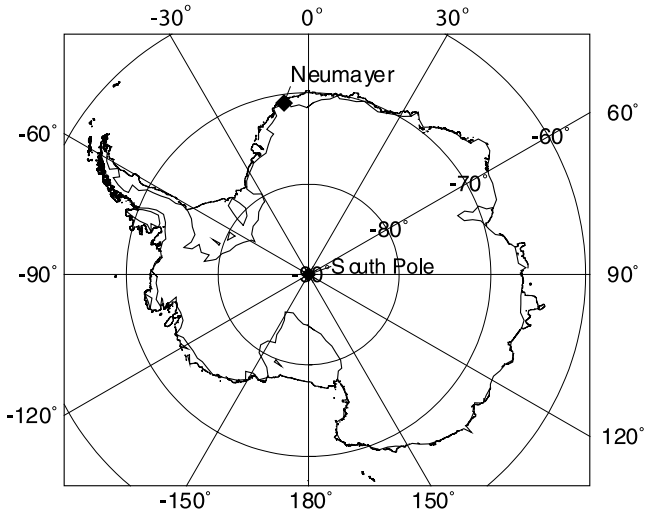

Figure 1. Locations of Neumayer Station and South Pole Station.

[13] Neumayer station is located on the Ekström Ice Shelf at a distance of 7 km from the southeast part of Atka Bay, 42 m above sea level. A detailed description of the location and its meteorology is given elsewhere [*König-Langlo et al.*, 1998]. The analysis of atmospheric HCHO was performed with a wet chemical fluorometric technique based on the so-called Hantzsch reaction [*Dong and Dasgupta*, 1987]. Hydrogen peroxide (H_2O_2) and methylhydroperoxide (CH_3OOH, also known as MHP) were analyzed with a two-channel enzymatic fluorimetry technique, developed by *Lazrus et al.* [1985]. For details on the measurement techniques, see *Riedel et al.* [1999, 2000].

[14] HCHO mixing ratios ranged from below detection limit (0.03 ppb, corresponding to 3 standard deviations of the noise level for an averaging time of 1 min) to 0.40 ppb in winter and 0.10 to 0.70 ppb in summer. H_2O_2 and MHP show mixing ratios of 0.20 ppb and 0.19 ppb, respectively, in summer and 0.05 and 0.09 ppb, respectively, in winter. The accuracy of the instrument was calculated to be of the order of 15–20% at [HCHO] $\leq$ 200 ppt and 10–15% at [HCHO] = 200–1000 ppt. The time constant for a change from 10 to 90% signal is 90 s with a delay time of 12 minutes [*Riedel et al.*, 1999].

[15] For comparison with the model results, we calculated monthly averages from our continuous measurements. Monthly averages represent the best comparison for our model calculations since we used mid month averages of radiation, CH_4, O_3, H_2O_2, and MHP to constrain the model and then allowed it to equilibrate over 30 days. The continuous time series show a large variability, which is reflected in the standard deviation of the average values. Monthly mean values and standard deviations for all three species are shown in Table 1. The detailed data are presented by *Riedel et al.* [1999, 2000]. The total measurement uncertainty is given by the instrumental accuracy, the efficiency in extracting the HCHO out of the air, and the calibration of the instrument. However, since we used monthly means for comparison with our model calculations, the standard deviation of this monthly mean is much larger than the instrument related uncertainties. Therefore we take the standard deviation given in Table 1 to be the uncertainty of the monthly mean.

2.2. Model Description

[16] Model calculations were performed with a simple zero-dimensional photochemical box model, referred to from now on as the National Institute of Water and Atmospheric Research (NIWA) model. This is based on a clean air subset of the Master Chemical Mechanism version 3 (MCMv3) developed at the University of Leeds, United Kingdom (available at http://mcm.leeds.ac.uk/MCM/). It includes 71 general gas-phase chemistry and photolysis reactions using MCMv3 rate constants derived from the International Union of Pure and Applied Chemistry database [*Atkinson et al.*, 2002] and the Jet Propulsion Laboratory [*Sander et al.*, 2003] database. This was extended to include isoprene, ethene, and propene oxidation using appropriate subsets of the MCMv3 reaction scheme. Modules for basic halogen and DMS chemistry were developed separately and incorporated when estimating possible effects of these reaction sets on HCHO concentrations (see Discussion). Emission and deposition processes for various significant species are also included, but no explicit heterogeneous chemistry schemes are incorporated.

[17] Diurnal variations of photolysis rates are based on functions in the MCMv3 model. Since these were derived for European mid-latitudes, MCM photolysis curves are not necessarily accurate at large solar zenith angles. Individual photolysis rate curves were examined and adjusted to high southern latitudes to match Antarctic conditions. Midday photolysis rates were normalized to the "J values" computed using the "4-stream" option of the Tropospheric Ultraviolet and Visible (TUV) radiative transfer model [*Madronich and Flocke*, 1998] for the location of Neumayer Station. The TUV model was constrained with observed ozone column densities at Neumayer Station and an estimated albedo of fresh snow of 0.95 [*Grenfell et al.*, 1994]. A cloud factor of 0.8 was applied to the clear sky TUV photolysis rates based on the observations of *Nichol et al.* [2003].

[18] The NIWA model was modified for high southern latitudes, including the effects of enhanced photolysis caused by stratospheric ozone depletion. We constrained the model with local observations of air temperature, total ozone column, water vapor pressure, and mixing ratios of

Table 1. Monthly Average and Standard Deviation of HCHO and Peroxide Measurements[a]

Month	HCHO, ppt	H_2O_2, ppt	MHP, ppt
January	388 ± 92	157 ± 87	165 ± 62
February	280 ± 138	154 ± 113	204 ± 105
March	152 ± 94	188 ± 97	144 ± 100
April	119 ± 71	57 ± 49	130 ± 72
May	212 ± 156	53 ± 41	89 ± 41
June	118 ± 83	76 ± 37	94 ± 44
July	98 ± 72	35 ± 20	62 ± 34
August	198 ± 137	43 ± 27	65 ± 23
September	308 ± 180	63 ± 73	75 ± 33
October	456 ± 171	206 ± 118	164 ± 51
November	479 ± 234	298 ± 147	191 ± 46
December	353 ± 227	230 ± 127	233 ± 139

[a]Data are from *Riedel et al.* [1999, 2000].

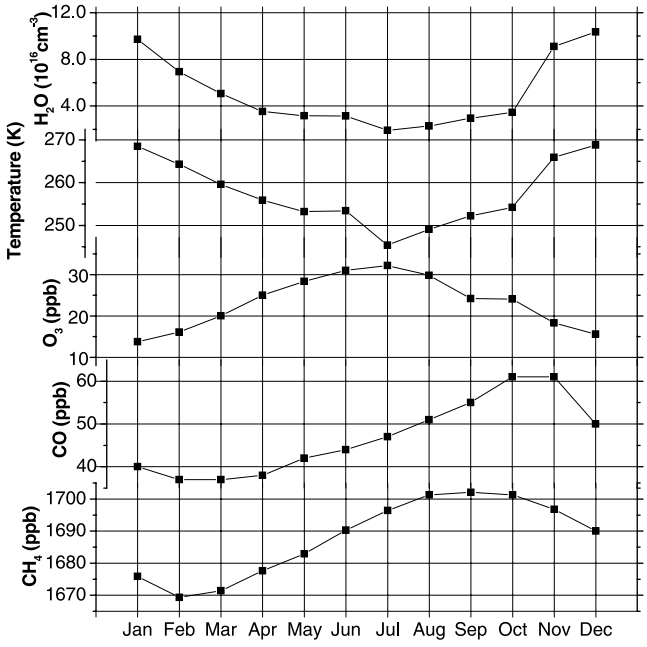

Figure 2. Monthly mean values of water content, temperature, tropospheric ozone, carbon monoxide, and methane measured at Neumayer and used as model input data.

CH_4, CO, NO_x ($NO + NO_2$), and tropospheric ozone. The input data that were used to constrain the model are depicted in Figure 2. CH_4, O_3, temperature, and humidity were routinely measured as part of the observation program at Neumayer Station. The water vapor pressure was calculated from relative humidity values with the empirical formula from *Marti and Mauersberger* [1993]. Seasonal CO mixing ratios were inferred from *Novelli et al.* [1994] (update: Figure 2.5 in Gas phase chemistry of the troposphere, by D. H. Ehhalt, in *Global Aspects of Atmospheric Chemistry*, edited by R. Zellner, Springer, New York, 1999) at 70°S. We included emission and deposition in the model and used parallel measurements of H_2O_2 and MHP in ambient air to further constrain the model. Measured photolysis rates and hydrocarbon concentrations would have greatly enhanced our model calculations but were unfortunately not available. A boundary layer height of 41.5 m was used as determined by airplane measurements at Neumayer Station in December 1997 [*Riedel*, 2001]. It was shown that boundary layer heights below 50 m are frequently observed in the vicinity of Neumayer [*Handorf et al.*, 1999]. Obviously, the boundary layer height will vary with meteorological conditions. During strong cyclonic events, the inversion layer vanishes completely and the boundary layer height becomes effectively infinite. During polar winter and at night when net radiation balance is negative, the Antarctic boundary layer is shallow and inversions reach a thickness of up to 2 km [*König-Langlo et al.*, 1998]. When considering HCHO fluxes out of the snow, the boundary layer height influences the total concentration of the HCHO. For example, the emission flux required to maintain a given concentration in the boundary layer scales directly with the boundary layer height. The fluxes presented in Figure 4 are calculated for 41.5 m. However, the boundary layer height variability introduces an uncertainty in our flux estimates that might account for some of the missing HCHO. It was pointed out by *Davis et al.* [2001] that shallow mixing depths in Antarctica can be responsible for unusually high mixing ratios.

[19] The standard height profiles of ozone and temperature in the model were adjusted to Antarctic conditions using measurements from balloon radio sondes launched as part of the meteorological program at Neumayer Station.

[20] Using a zero-dimensional model always means that transport processes are not accounted for. We believe that this is acceptable since in this paper we will concentrate on the times during the year (late spring, summer, and early autumn), when atmospheric composition at Neumayer is largely dominated by local photochemistry [*Riedel*, 2001]. It was shown by *Riedel* [2001] that during the polar night, local photochemistry dies down and long-range transport dominates the effective mixing ratios at Neumayer during winter. Long-range transport of peroxides (or peroxide precursors) from sunlit regions becomes possible due to increased lifetimes ($\tau_{\text{polar night}}(H_2O_2) \approx 7$d) [*Riedel et al.*, 2000]. However, in daylight peroxide lifetime decreases ($\tau_{\text{polar day}}(H_2O_2) \approx 3$d) [*Riedel et al.*, 2000], and long range transport becomes less likely. Moreover, atmospheric mixing ratios are more uniform during summer, and peroxide concentrations over the South Pacific and South Atlantic do not vary considerably from those at Neumayer [*Junkermann and Stockwell*, 1999; *O'Sullivan et al.*, 1999; *Weller et al.*, 2000].

[21] Though these points were made for peroxides, it is likely that they are also valid for HCHO and its precursors. The lifetime of HCHO in the polar night is extremely long ($\tau_{\text{polar night}}(\text{HCHO}) = 120$ days [*de Serves*, 1994]), while during the day it is of the order of a few hours [*Palmer et al.*, 2003], suggesting that long-range transport during the polar night is very likely but is negligible during the sunlit period of the year.

[22] Another aspect of transport processes is down-mixing of free tropospheric air. HCHO profiles in the remote marine troposphere were determined by aircraft measurements, and showed that HCHO decreases with increasing altitude [*Singh et al.*, 2000; *Frost et al.*, 2002; *Wert et al.*, 2003]. HCHO mixing ratios in the free troposphere seem to be lower than in the marine boundary layer, due to (1) lower water vapor concentration leading to lower OH mixing ratio, (2) lower temperatures decreasing the rate constant for the reaction of OH with CH_4, and (3) increased J-values leading to increased HCHO photolysis. This assumes that increased sink processes in the marine boundary layer are not operative to cancel this effect. Therefore, we can rule out that down-mixing from the free troposphere to the surface is responsible for the increased HCHO levels discussed in this study [*Junkermann and Stockwell*, 1999; *Weller et al.*, 2000].

3. Results

[23] The NIWA model was run in two different ways. We ran it first without any deposition or emission fluxes to calculate the contribution of CH_4 gas-phase photochemistry to the HCHO budget. The simulations were constrained by

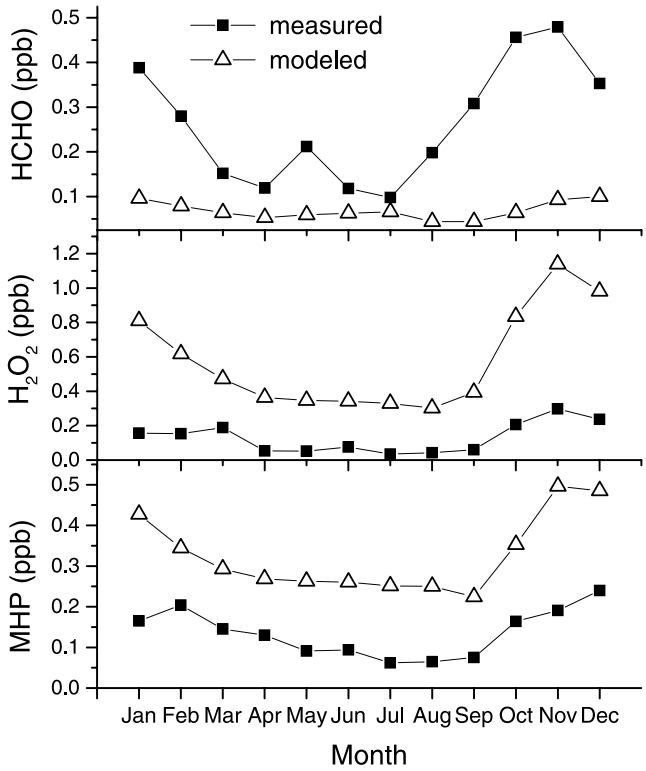

Figure 3. Comparison of measured and modeled monthly mean values of HCHO, H_2O_2, and MHP, with only methane oxidation included in the model.

observational data for CH_4, CO, O_3, temperature, and calculated water vapor pressure (Figure 2). NO_x (NO and NO_2) was only measured during the Photochemical Experiment at Neumayer (PEAN) in February 1998 with a mean value of 6 ppt [*Jones et al.*, 1999]. We adjusted the model input of N-containing species in February to match these observations. Since no NO_x measurements were available during the rest of the year, we varied input NO_x depending on light intensity using the $j(NO_2)$ photolysis rate derived from TUV as a scale factor. Our NO concentrations are comparable to measured NO mixing ratios ranging from $\leq$1 ppt in June up to $\leq$7 ppt in December [*Weller et al.*, 2002]. Since NO concentrations can dramatically affect HCHO production rates, continuous measurements of NO would be desirable for future measurement campaigns. However, we are confident that pollution plumes did not influence HCHO concentrations since the air chemistry observatory, where HCHO was measured, is located in a clean air sector 1500 m south of the main station and northerly winds are hardly ever observed [*König-Langlo et al.*, 1998]. Hydroperoxide mixing ratios were unconstrained during this model run (Figure 3). Additional measurements of isoprene, ethene, and propene would significantly help to constrain the model and improve our results.

[24] Since we are concerned only with comparing model results with monthly means of the observational data, the model was run for 30 diurnal cycles using the input conditions for this particular month. The diurnal mean output values of the last cycle were then used for comparison with the observational data for this month. During months when the Sun is relatively high above the horizon, photolysis rates are large and the system comes quickly to chemical equilibrium. However, during months when photolysis rates are low or nearly zero, equilibrium is not achieved in 30 days. Our procedure was to begin with February when equilibrium was quickly achieved and NO_x measurements were available. We then initialized each succeeding month with the previous month's result. This ensured that the monthly values obtained during winter and near winter conditions were connected consistently to earlier months. We closed the procedure by checking that the initial February output values were obtained again when the second February was reached.

[25] Comparison of HCHO, H_2O_2, and MHP measurements with model results (Figure 3) reveals that basic gas-phase photochemistry alone cannot explain the observed mixing ratios. Our model underestimates the observed HCHO values, especially in spring and summer when model predictions are 90–100 ppt HCHO and observations are 350–470 ppt. This large magnitude and the higher variability in HCHO mixing ratios during summer, as indicated by the higher standard deviation (see Table 1), most likely reflect a higher variability in surface sources and factors influencing HCHO emissions, which will be discussed in section 4.1. During this model run the calculated H_2O_2 and MHP mixing ratios were unrealistically high, since deposition as a sink was neglected, and hydroperoxides were only removed from the atmosphere by photochemistry.

[26] In the next step we reran the NIWA model including simultaneous deposition of hydroperoxides and emission of HCHO. We used the measured H_2O_2, MHP, and HCHO mixing ratios to constrain our model and adjust the deposition and emission fluxes. The results are shown in Figure 4a. H_2O_2 deposition flux peaks in November (20.6×10^{12} molecules m^{-2} s^{-1}) and is lowest in June, when a very small emission flux ($-0.016 \times$

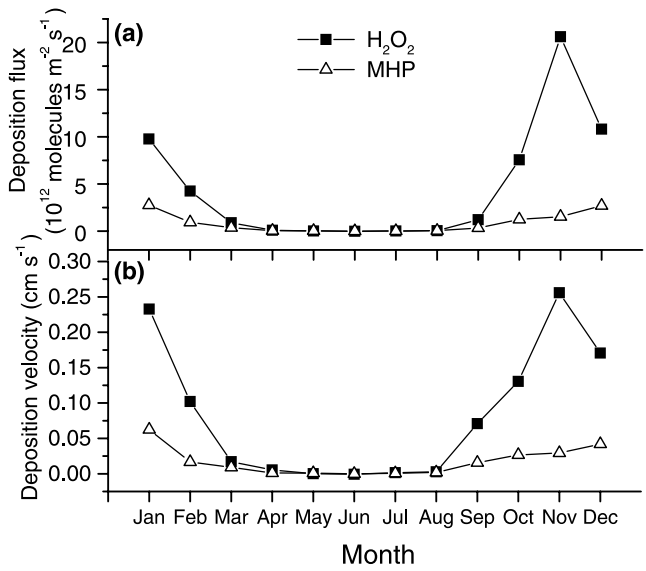

Figure 4. (a) Modeled peroxide deposition fluxes and (b) deposition velocities for Neumayer.

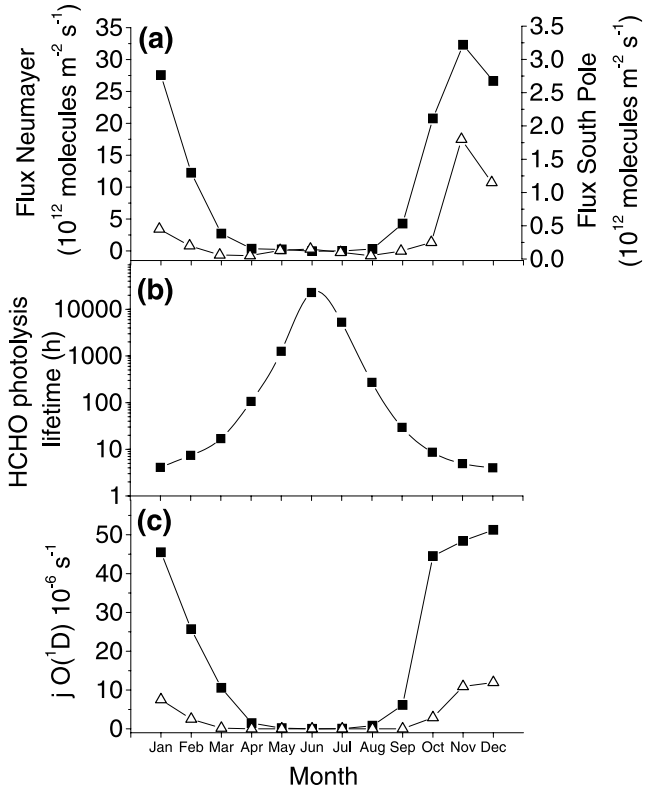

Figure 5. (a) HCHO flux modeled for Neumayer Station and estimated for South Pole from modeling of firn equilibration with air [*Hutterli et al.*, 2002]. Note the different scales on both *y* axes. (b) Modeled HCHO lifetime to photolysis. (c) Photolysis rate from the Tropospheric Ultraviolet and Visible (TUV) model for $O(^1D)$ at Neumayer (70°S) and South Pole (90°S).

10^{12} molecules m^{-2} s^{-1}) is needed to match observations. A flux of this size is most likely not physically significant. The maximum MHP deposition flux (2.75×10^{12} molecules m^{-2} s^{-1}) is 10 times smaller than the maximum H_2O_2 flux and appears in January. In June neither emission nor deposition flux is needed to match MHP measurements in this model run (Figure 4).

[27] The calculated deposition fluxes are dependent on the atmospheric peroxide mixing ratios. An independent variable is the dry deposition velocity, which is obtained by dividing the deposition flux by the atmospheric peroxide concentration at the time. Model-derived deposition velocities are shown in Figure 4b. The H_2O_2 deposition velocity is greatest in November (0.26 cm s^{-1}), while for MHP the maximum is in January (0.06 cm s^{-1}). Previous model results found peroxide dry deposition velocities of 0.32 cm s^{-1} for H_2O_2 over ice [*Hauglustaine et al.*, 1994] and 0.05 cm s^{-1} for MHP over ice [*Hough*, 1991]. Both values agree with our derived maximum deposition velocities.

[28] To match our HCHO observations, we had to include HCHO emissions of up to 3.2×10^{13} molecules m^{-2} s^{-1} (in November) (Figure 5a). In June and July we calculated minor deposition fluxes (4.2×10^{10} and 4.6×10^{9} molecules m^{-2} s^{-1}, respectively) into the snow. Note that the biggest HCHO emission flux is needed in November when ozone depletion in Antarctica reaches a maximum due to photolysis.

[29] Photolysis is the major sink for HCHO in summer. With bigger solar zenith angles this sink becomes less important. Figure 5b shows the modeled HCHO photolytic lifetime throughout the year, as derived from mean daily J-values relevant to HCHO in the month concerned. Note the logarithmic axis. The lifetime varies from about 4 hours in December to about 2.5 years in June. The summer value is consistent with a calculated turnover time of 5 hours in November balancing the loss of HCHO due to photolysis with the necessary flux and the previously used boundary layer height of 41.5 m.

[30] A good indication that primarily photochemical reactions influence the atmospheric concentrations of HCHO is the occurrence of definite diurnal variations. However, at Neumayer a diurnal cycle is seldom observed and is only apparent during good weather conditions, that is, wind speeds below 10 m s^{-1} and no precipitation or drifting snow [*Riedel et al.*, 1999; *Riedel*, 2001]. When diurnal cycles were observed, highest HCHO mixing ratios occurred in the early afternoon (around 2 pm), lowest after midnight. At the end of October the maximum HCHO mixing ratio was 0.65 ppb in the early afternoon, and the lowest was 0.30 ppb during the night. The average concentration during this time was 0.45 ppb.

[31] Since these diurnal cycles are rare and nonrecurring, we assume that photochemical effects generally exist, but are commonly masked by meteorological effects. Our model calculations reveal a diurnal cycle for HCHO in October and November that is similar to the observed one. While variation of the boundary layer height in the model offsets the HCHO background, leaving the amplitude of the diurnal cycle the same, an increase in cloud factor, representing a clear day, leads to a larger diurnal amplitude.

4. Discussion

[32] Our model calculations show that basic photochemistry alone cannot explain observed HCHO mixing ratios at Neumayer Station. We must assume there is a HCHO source that is not yet included in our photochemical model. By constraining the model with meteorological and trace gas data, especially with hydroperoxide measurements, we feel confident that we have quantified the size of the unknown source. As a first approximation, we called the source a "HCHO emission flux". This does not necessarily mean that we are dealing with one uniform source or that this source is actually a direct emission. In the following subsections, we will discuss possible contributions to this "emission flux".

[33] In the rest of this paper, we focus on the month of November when the measured monthly average HCHO mixing ratio was largest, at 479 ppt. When running the NIWA model from now on, we constrain the following species to their observed values: CH_4, 1697 ppb; CO, 61 ppb; O_3, 18 ppb; H_2O_2, 298 ppt; MHP, 191 ppt. Although we have no NO_x measurements in November, we expect NO_x mixing ratios to be in the range 5–10 ppt [*Jones et al.*, 1999; *Weller et al.*, 2002]. Since HCHO production from CH_4 and other hydrocarbons is very sensitive to NO_x

changes under low NO_x conditions, we run the model for mean daily NO_x mixing ratios of both 5 and 10 ppt.

[34] With the above constraints under Neumayer November photolysis conditions, we found that the HCHO mixing ratios produced from CH_4 alone were 49–67 ppt in the NO_x range 5–10 ppt. From now on, when ranges of HCHO mixing ratios or percentage changes are quoted, they will refer to the NO_x range 5–10 ppt. This also applies to ranges quoted for other species.

4.1. Emission From the Snow Surface

[35] Previous investigations in the Arctic revealed strong interaction with the snow surface. Several processes may be involved in the exchange between snowpack and atmosphere [*Dominé and Shepson* 2002, and references therein] such as adsorption, solid-state diffusion and co-condensation. Apart from these purely physical processes, chemical reactions can also take place, either initiated by light or by temperature or both. It seems that the mechanism depends on both physical and chemical conditions and may also vary significantly from one site to another [*Dominé and Shepson*, 2002]. Two established explanations for HCHO are emissions from buried HCHO rich winter snow layers [*Hutterli et al.*, 1999], and photolysis of the nitrate ion (NO_3^-) that produces condensed phase OH radicals, which then react with dissolved organic matter in the snow [*Grannas et al.*, 2002; *Sumner et al.*, 2002]. If the first mechanism takes place, a correlation between temperature and emissions should be observable since the relevant processes, like adsorption and diffusion, are temperature dependent. If photolysis causes HCHO emissions, a correlation with light (in particular ultraviolet (UV) radiation) should be detected.

[36] Recent laboratory investigations have indeed revealed that carbonyls are produced by irradiating snow [*Grannas et al.*, 2004]. Arctic (Greenland, Canada) and Antarctic snow samples were irradiated, and HCHO production was observed. Snow samples were also analyzed for dissolved organic carbon. The total amount of carbon (TOC) varies with season. Arctic snow had 0.58–0.70 mg l^{-1} in spring and summer and 0.2–0.4 mg l^{-1} TOC in fall and winter [*Grannas et al.*, 2004]. Higher carbon contents of 1.85 mg l^{-1} were found during field experiments at Summit in the summers of 1999 and 2000 [*Dassau et al.*, 2002]. TOC in Antarctic snow was lower, 0.5 mg l^{-1} in April and October and 0.1 mg l^{-1} in January and July (A. M. Grannas, personal communication, 2003). The proximity of ice-free landmasses and industrialized countries together with Russian rivers that drain into the Arctic Ocean, supplying large amounts of organic material, can explain higher TOC in Arctic snow samples.

[37] Nitrate levels were also determined. For Alert and Summit snow samples, NO_3^- levels were typically around 1×10^{-6} mol l^{-1} (A. M. Grannas, personal communication, 2003). Typical nitrate concentrations at Neumayer base are 0.8×10^{-6} mol l^{-1} (50 ppb) [*Jones et al.*, 2000] compared with South Pole values of 1.9×10^{-6} mol l^{-1} NO_3^- [*Dibb and Whitlow*, 1996]. Since both TOC and NO_3^- levels are higher in Arctic than in Antarctic snow, higher radical production and therefore higher HCHO emissions from Arctic snow can be expected.

[38] Recent HCHO flux measurements at Summit, Greenland, reported an average net emission flux of $(7^{+12.6}_{-12.2}) \times 10^{16}$ molecules m^{-2} per day [*Jacobi et al.*, 2002]. This translates to 0.8×10^{12} molecules m^{-2} s^{-1}. The maximum emission flux measured during this study was 4.2×10^{12} molecules m^{-2} s^{-1} around noon [*Jacobi et al.*, 2002]. Note that during night HCHO deposition was observed. Likewise, HCHO emission flux estimates from HCHO measurements in firn air at Summit using a gas transfer model are $1.4–8 \times 10^{12}$ molecules m^{-2} s^{-1} [*Hutterli et al.*, 1999]. These results are of the same order of magnitude though the different techniques show slightly different results, which may be due to different sampling years. However, if we assume that processes similar to those in the Arctic are responsible for HCHO emissions out of Antarctic snow, we would expect similar but somewhat smaller emissions due to lower TOC. Comparison with the maximum HCHO flux (32×10^{12} molecules m^{-2} s^{-1}) that we derived to match our November Neumayer observations, shows that our modeled fluxes are 4–40 times bigger than measured in the Arctic.

[39] A gas transfer model was also used to calculate HCHO fluxes from firn air measurements at South Pole [*Hutterli et al.*, 2002]. Figure 5a compares Neumayer and South Pole HCHO fluxes. Calculated HCHO emissions at Neumayer are 20 to 60 times higher than at South Pole (note the different ordinate scales in Figure 5a). We will investigate UV radiation and temperature differences at both stations as possible reasons for these different fluxes.

[40] UV radiation: Because of its proximity to the pole, South Pole Station gets less UV radiation than Neumayer. If HCHO production is directly dependent on UV radiation, smaller HCHO emissions at South Pole are likely. Since no direct radiation measurements were available, we used TUV to derive the $O_3 \rightarrow O(^1D) + O_2$ photolysis rate. We compared the ozone photolysis rates for South Pole and Neumayer (Figure 5c). The largest differences in ozone photolysis rates appear in March and September (60 to 240 times) when Neumayer experiences sunlight and South Pole is still dark. In summer, Neumayer ozone photolysis rates are 4 to 5 times larger than at South Pole. However, during this period 60 times larger HCHO fluxes were inferred from the NIWA model to produce the observed HCHO mixing ratio. Though photolysis rate and emission of HCHO are not linearly related, we consider that differences in UV radiation can only partly explain the larger HCHO emission fluxes at Neumayer.

[41] Temperature: If HCHO is produced from OH generated from nitrate in the snowpack, then the OH quantum yield is temperature dependent [*Chu and Anastasio*, 2003]. The average temperature at Neumayer is −16.1°C [*König-Langlo et al.*, 1998], typically more than 30°C warmer than South Pole (−49.3°C). This can easily account for a factor of 2 in OH production, in addition to the higher actinic fluxes discussed in the previous section. If on the other hand, HCHO emissions are related to release from HCHO enriched winter layers, then again a higher average temperature at Neumayer will foster higher HCHO emissions. Additionally, due to its proximity to the coast Neumayer has also much higher snowfall than South Pole so that the HCHO-rich winter layer is probably much thicker. All these

factors have very high uncertainties leading to a rather substantial uncertainty in likely HCHO emissions.

[42] Nevertheless, the modeled HCHO fluxes required to match observations at Neumayer are higher than any estimated or measured fluxes for polar regions [*Hutterli et al.*, 1999, 2002; *Jacobi et al.*, 2002].

4.2. DMS as HCHO Precursor

[43] Dimethylsulfide (DMS) is produced in the marine biosphere through phytoplankton activity. It is emitted to the water and can enter the atmosphere by mixing and ocean-atmosphere exchange. Equilibrium concentrations in the water are several orders of magnitude larger than air concentrations. Therefore DMS is permanently emitted to the atmosphere. DMS fluxes are dependent on wind velocity (influencing turbulence) and temperature (influencing the solubility of the gas). In the atmosphere, DMS is oxidized by OH radicals. In this process H can either be abstracted from or added to DMS. The effective branching ratio is temperature dependent. At a temperature of 1.4°C, approximately 65% of the DMS is oxidized by addition and 35% is oxidized by abstraction [*Hynes et al.*, 1986]. If abstraction takes place, followed by reaction with oxygen and NO, HCHO can be produced [*Yin et al.*, 1990]:

[44] The rate-limiting step in this process is the reaction with NO. The yield of HCHO from this reaction was found to be 1.04 ± 0.13 [*Urbanski et al.*, 1997]. The overall yield is therefore only dependent on the initial branching ratio.

[45] DMS has previously been considered as a HCHO precursor [*Ayers et al.*, 1997], though in that study the authors considered the amount of HCHO produced from DMS to be negligible. It must be emphasized that they based their conclusion on model results obtained with an atmospheric DMS concentration measured in summer at Cape Grim (41°S) of 122–147 ppt. The estimated monthly average DMS flux from the ocean surface was 3.5×10^{13} molecules m^{-2} s^{-1} [*Ayers et al.*, 1995].

[46] However, recent investigations by *Curran and Jones* [2000] estimated DMS fluxes in the range $1.2–34.2 \times 10^{13}$ molecules m^{-2} s^{-1} from DMS measurements in seawater in the Australian sector of the Southern Ocean using the method of *Liss and Merlivat* [1986]. Highest concentrations (7.9 nM) were found in the seasonal ice zone close to the continental margins in January. On the basis of this DMS seawater concentration, a flux of 34.2×10^{13} molecules m^{-2} s^{-1} was calculated, 10 times larger than the flux that *Ayers et al.* [1995] estimated, even though the former flux does not include potential contributions from sea ice. Moreover, the *Liss and Merlivat* [1986] flux calculation method represents the lower end of a range of flux calculation methods so that it is possible that the *Curran and Jones* [2000] fluxes are still underestimates. High DMS concentrations in Antarctic waters were also observed by other studies. At the French station Dumont d'Urville (66°40′S, 140°01′E) in the Pacific Ocean sector and on the opposite side of the Antarctic continent to Neumayer, a huge amount (57 ± 23 nM) of DMS was present in early January [*Jourdain and Legrand*, 2001]. This event was accompanied by high atmospheric DMS levels (855 ppt). The largest atmospheric mixing ratios were observed during a day in December when 2790 ppt DMS were present [*Jourdain and Legrand*, 2001]. At Palmer Station on the Antarctic Peninsula, atmospheric DMS mixing ratios of 6–595 ppt were observed in January and February 1994 [*Berresheim et al.*, 1998]. Seawater concentrations ranged from 0.7 to 3.7 nM. The corresponding fluxes based on the method of *Liss and Merlivat* [1986] are $0.02–13.38 \times 10^{13}$ molecules m^{-2} s^{-1}. Atmospheric DMS measurements during a cruise from Australia to the Japanese Antarctic Station Syowa were up to 420 ppt DMS [*Yokouchi et al.*, 1999]. DMS measurements from Neumayer only exist for 1992 [*Kleefeld*, 1998]. The highest DMS concentration measured in air was 74.5 ppt and 1.1 nM in seawater.

[47] From all these studies it is clear that DMS concentrations are higher than previously expected in Antarctic regions. Occasionally, extremely high levels occur. Such events were always connected with either phytoplankton blooms [*Berresheim et al.*, 1998] or very high chlorophyll content [*Jourdain and Legrand*, 2001]. Since DMS production is connected with phytoplankton activity this is not surprising, but it also allows us to reverse the process and use chlorophyll to predict the existence of likely DMS fluxes. Chlorophyll content can be derived from satellite observations (available from the World Wide Web site http://seawifs.gsfc.nasa.gov). We analyzed weekly Seaviewing Wide Field-of-view Sensor (SeaWiFS) pictures for November, December, and January, and two focal points emerged. First, regions close to the ice shelf showed high chlorophyll content (1 to 3 mg m^{-3}) though the ocean was covered with sea ice. These regions can be related to polynyas (open ice-free water) and demonstrate that DMS emissions can even occur during the Antarctic winter and early spring due to these open water areas. Secondly, chlorophyll content increases dramatically with the break up of the sea ice, which can explain highly elevated DMS levels during this time of the year (December and January).

[48] We performed preliminary calculations using the NIWA model with no direct HCHO emission, but including a module for oxidation of DMS in the marine boundary layer, modified to simulate Neumayer conditions [*de Bruyn et al.*, 2002; J. M. Cainey, personal communication, 2003], and applying the proposed DMS fluxes of $1.2–34.2 \times 10^{13}$ molecules m^{-2} s^{-1} [*Curran and Jones*, 2000]. For a flux of 1.2×10^{13} molecules m^{-2} s^{-1} our model predicts atmospheric HCHO mixing ratios of 54–71 ppt, a 10–6% increase over CH_4 alone. The DMS mixing ratios are around 200 ppt. This result shows that HCHO concentrations in the air increase if there are large DMS fluxes. If we assume a DMS flux of 34.2×10^{13} molecules m^{-2} s^{-1}, we obtain 121–160 ppt HCHO, an increase of about 140% over CH_4 alone. The corresponding DMS mixing ratio is 6600 ppt. Such high atmospheric DMS mixing ratios have not been observed in Antarctica (the maximum being 2770 ppt at Dumont d'Urville [*Jourdain and Legrand*, 2001]). However, it is clear that even very high DMS mixing ratios fall well short of providing enough HCHO to explain the observed mean November HCHO mixing ratio at Neumayer.

4.3. Isoprene as HCHO Precursor

[49] In continental regions isoprene (C_5H_8), a biogenically produced hydrocarbon, is known to be a significant precursor of HCHO [*Sprengnether et al.*, 2002]. The oxi-

dation of isoprene by OH produces HCHO in a fractional yield of 0.63 [*Carter and Atkinson*, 1996].

[50] In the marine boundary layer, isoprene has so far been considered to be negligible [*Ayers et al.*, 1997]. However, recent investigations have shown that marine biogenic isoprene sources exist [*Broadgate et al.*, 1997; *Yokouchi et al.*, 1999; *Shaw*, 2001]. These are strongly correlated with the chlorophyll content of the water indicating that phytoplankton activity is the most likely source for marine isoprene. With an averaged flux of 2.2×10^{11} molecules m^{-2} s^{-1} in spring [*Broadgate et al.*, 1997], marine sources are smaller than terrestrial sources but can probably affect local photochemistry in the remote marine boundary layer.

[51] During a Japanese cruise in austral summer 1997/1998, from Australia to the Japanese Antarctic Station Syowa, isoprene mixing ratios up to 57 ppt (average: 13 ppt) were measured over the Southern Ocean [*Yokouchi et al.*, 1999]. Highest concentrations occurred south of 45°S.

[52] At Cape Grim, Tasmania, isoprene was measured in January and February 1999 as part of the Second Southern Ocean Photochemistry Experiment (SOAPEX 2). Though isoprene concentrations were most of the time influenced by the local terrestrial biomass (eucalyptus, grass), diurnal cycles with isoprene midday maximums of up to 8 ppt during identified periods of baseline marine airflow from Southern Ocean regions were observed [*Lewis et al.*, 2001].

[53] During a recent measurement campaign at the British Antarctic station Halley, 20–30 ppt of ethene were observed year-round with no obvious seasonal cycle (perhaps a little more in summer). Propene mixing ratios were at the detection limit of the instrument, (~10 ppt) with no significant seasonal cycle. Isoprene mixing ratios were not above the detection limit of the instrument (~5 ppt) at any point in the year (A. Lewis, personal communication, 2005).

[54] In order to investigate the contribution of small amounts of marine isoprene we included a module in the NIWA model based on the MCMv3 isoprene system. Model runs for Neumayer November conditions showed that 10 ppt of isoprene in the Antarctic troposphere could produce 16–19 ppt (33–28%) increases in HCHO over that generated by CH_4 oxidation This is consistent with *Ayers et al.* [1997], who estimated that ~10 ppt of isoprene could produce HCHO equivalent to 30% of that from CH_4 oxidation. An isoprene mixing ratio of 60 ppt (consistent with the larger values measured by *Yokouchi et al.* [1999]) leads to increases of 74–85 ppt HCHO (151–127%) over that generated by CH_4.

[55] Although 60 ppt of isoprene produces a significant increase in HCHO, it is clearly insufficient to explain the 479 ppt of HCHO measured. In further model runs, we determined the amount of isoprene required to match the HCHO observed at Neumayer in November. The model predicts more than 600 ppt of isoprene, an amount that is extremely unlikely to be present in the Antarctic troposphere.

4.4. Ethene and Propene as HCHO Precursors

[56] The photooxidation of various hydrocarbons produces HCHO, but not all hydrocarbons have the same potential to produce HCHO. For normal alkanes (C_nH_{2n+2}), HCHO molar yields are typically between 0.1 and 0.3 (exceptions are methane with 1.0 and isobutane with 0.8 [*Wert et al.*, 2003]). For unsaturated hydrocarbons (alkenes, C_nH_{2n}), these yields are much higher, 1.6 for ethene (C_2H_4) [*Niki et al.*, 1981] and 1.0 for propene (C_3H_6) [*Niki et al.*, 1978]. We will focus on these two hydrocarbons since higher alkenes are hardly found in the remote marine boundary layer.

[57] So far, most investigations on alkenes in polar regions have been performed in the Arctic. Environmental conditions in the Arctic are slightly different from the Antarctic since the Arctic is surrounded by highly industrialized countries. As a consequence, anthropogenic emissions including various hydrocarbons are much higher in the Arctic, a circumstance that complicates comparison.

[58] At Alert, Canada, ethene ambient air mixing ratios of 10 to 100 ppt were observed in April [*Bottenheim et al.*, 2002]. Gradient and flux measurements performed during this study suggest that the snowpack is a possible source of ethene, reflected in a flux estimate of 1×10^{11} molecules m^{-2} s^{-1} ethene from the snow to the atmosphere [*Bottenheim et al.*, 2002]. Measurements of ethene in ambient and firn air at Summit, Greenland, showed surprising results. While ethene mixing ratios in air were between 3 and 10 ppt, firn air 10 cm deep in the snowpack contained between 40 and 260 ppt revealing also a distinct diurnal cycle with the maximum concentration at 14:00 and the minimum at 2:00 [*Swanson et al.*, 2002]. This suggests that light strongly influences the production of ethene, an assumption supported by snow-chamber experiments showing higher alkene mixing ratios when the snow is irradiated [*Swanson et al.*, 2002]. Production rates of 1.7×10^6 and 1.2×10^6 molecules cm^{-3} s^{-1} of ethene and propene, respectively, were calculated [*Swanson et al.*, 2002]. The origin of the ethene and propene found in firn air is likely to be photochemical production from organic material in the snow, a process that is already known to occur when seawater is irradiated [*Riemer et al.*, 2000]. In contrast to isoprene, alkene emissions show no strong correlation with chlorophyll content in the water [*Shaw*, 2001], indicating that photolysis of dissolved organic carbon (DOC) is the more likely source. Substantial localized oceanic sources for ethene and propene were also suggested by *Hopkins et al.* [2002], and *Blake et al.* [1996] found up to 100 ppt ethene immediately over the ocean surface.

[59] The only ambient air measurements in the Southern Hemisphere to be found in literature were performed at Cape Grim, Tasmania, detecting up to 15 ppt ethene and 7.5 ppt propene [*Lewis et al.*, 2001] in the marine boundary layer. Earlier measurements at Neumayer Station, Antarctica, by *Rudolph et al.* [1989] revealed extremely high ethene and propene mixing ratios due to artifacts as a consequence of long storage in stainless steel canisters.

[60] Since no other alkene measurements were available for Neumayer, we assumed the same mixing ratios as *Ayers et al.* [1997] of ~45 ppt ethene and ~15 ppt propene in the marine boundary layer. We included MCMv3 ethene and propene chemistry reactions in the NIWA model and performed two separate runs. We found that 45 ppt ethene produce 4.8–5.4 ppt (10–8%) additional HCHO, while 15 ppt propene produce 3.7–4.8 ppt (7.5–7%) additional HCHO. For ethene and propene together, we therefore

calculated an HCHO increase of 8.5–10.2 ppt (17.5–15%), which is comparable with the ~10% estimate of *Ayers et al.* [1997]. These findings are also confirmed by our earlier calculations [*Riedel*, 2001] with the Harvard photochemical box model [e.g., *Schultz et al.*, 1999] that showed an increase in HCHO of about 13% with the same ethene and propene mixing ratios. Thus unrealistically large ethene and propene mixing ratios would be required at Neumayer to give the observed HCHO mixing ratios.

4.5. Halogen Chemistry

[61] Photochemically produced OH radicals usually dominate the fate of trace gases such as CH_4 and NMHCs in the daytime troposphere. However, in the remote marine boundary layer halogens like chlorine (Cl) and bromine (Br) can contribute significantly to local photochemistry, a fact that is often neglected in photochemical models.

[62] In recent years, oxidation by the highly reactive chlorine atom has gained much attention. *Spicer et al.* [1998] showed that Cl_2 is elevated in the marine boundary layer. They measured < 10 to 150 ppt Cl_2, an order of magnitude more than predicted for marine air. The early morning photolysis of Cl_2 forms Cl (up to 1.3×10^5 molecules cm^{-3}) and leads to an enhanced oxidation of hydrocarbons. Since the reaction of Cl with hydrocarbons is in most cases faster than the reaction with OH, the two reactions can compete with each other, even when Cl mixing ratios are lower than OH levels. The reaction of CH_4 with Cl produces HCHO in significant amounts via the following reaction sequence:

(R4) $$CH_4 + Cl \rightarrow CH_3 + HCl$$

(R5) $$CH_3 + O_2 \rightarrow CH_3O_2$$

(R8) $$CH_3O_2 + NO + O_2 \rightarrow HO_2 + NO_2 + HCHO$$

[63] Calculations with the MOCCA model showed that Cl atom levels higher than 1×10^5 atoms cm^{-3} (daily maximum) have a substantial impact on HCHO concentrations [*Wagner et al.*, 2002]. The number of Cl atoms available is crucial since 1×10^5 atoms cm^{-3} increase HCHO mixing ratios by 22% and 5×10^5 atoms cm^{-3} double HCHO compared to a run with no Cl oxidation [*Wagner et al.*, 2002].

[64] In the literature, Cl atom concentrations in the marine boundary layer between 1.0×10^3 molecules cm^{-3} and 1.3×10^5 molecules cm^{-3} were calculated based on measurements of hydrocarbons during ozone depletion events [*Jobson et al.*, 1994; *Rudolph et al.*, 1999; *Boudries and Bottenheim*, 2000] and from measurements of $\delta^{13}C$ in CH_4 [*Allan et al.*, 2001]. *Fried et al.* [2003b] give an upper limit of 5×10^5 atoms cm^{-3} to give an identical production rate of HCHO from the reaction of CH_4 with OH. The assumed Cl atom concentration of 5×10^5 atoms cm^{-3} by *Wagner et al.* [2002] is probably at the upper limit for Cl concentrations in the marine boundary layer. However, enhanced Cl concentrations will increase HCHO production.

[65] The effect of Br on HCHO is quite different from Cl. While Cl can react with CH_4, the reactivity of Br is only sufficient to abstract hydrogen atoms from HO_2 and aldehydes [*Seinfeld and Pandis*, 1998]. The rate constant for the reaction between HCHO and Br is relatively fast, so that Br may be a significant sink for HCHO.

(R6) $$Br + HCHO \rightarrow HBr + CHO$$

(R7) $$BrO + HCHO \rightarrow HOBr + CHO$$

[66] The importance of the second reaction was especially emphasized by *Michalowski et al.* [2000], since this reaction represents an important sink not only for HCHO but also for BrO, which has an important influence on the Br chemistry. However, Br can also produce HCHO through the following reaction:

(R9) $$BrO + CH_3O_2 \rightarrow Br + HCHO + HO_2$$

As a consequence of reactions (6), (7), and (9), elevated levels of Br possibly do not increase HCHO levels, and may even decrease them [*Michalowski et al.*, 2000]. Note, however, that the importance of reaction (7) is contentious. *Hansen et al.* [1999] reported a rate coefficient of 1.5×10^{-14} cm^3 $molecule^{-1}$ s^{-1} for this reaction. *Orlando et al.* [2000] found no conclusive evidence for the occurrence of the reaction, and suggested an upper limit for the rate coefficient of less than 4×10^{-15} cm^3 $molecule^{-1}$ s^{-1}, perhaps significantly less at polar tropospheric temperatures.

[67] The importance of Cl and Br in tropospheric ozone depletion events during polar sunrise has been clearly demonstrated [*Ridley et al.*, 2003, and references therein]. *Sumner and Shepson* [1999] showed that during these ozone depletion events variations in HCHO mixing ratios could be observed. An anti-correlation between O_3 and HCHO was detected for O_3 concentrations between 10 and 20 ppt. The lower the O_3, the higher the HCHO. This changed when O_3 mixing ratios dropped to zero, since then also HCHO decreased drastically. A reason for this behavior was given by *Rudolph et al.* [1999]. In times of moderate O_3 destruction more Cl than Br atoms are available, and HCHO production is increased due to the reaction of Cl with CH_4. When O_3 is totally destroyed, the concentration of Br increases to a level when HCHO is destroyed by the reaction with Br.

[68] For our own calculations with the NIWA model, we used a module with simplified halogen production and chemistry based on the work of *Lehrer et al.* [2004] and U. Platt (manuscript in preparation, 2005). As halogen input concentrations, we assigned a Cl concentration of 5×10^3 atoms cm^{-3} and a Br concentration of 1.5×10^6 atoms cm^{-3}. These concentrations are based on a study of the available literature [*Wagner et al.*, 2002; *Boudries and Bottenheim*, 2000; *Rudolph et al.*, 1999; *Jobson et al.*, 1994; U. Platt, personal communication, 2004].

[69] We ran the model with Cl and Br chemistry under Neumayer November conditions. The measured mean O_3

mixing ratio of 18 ppb was used, so that O_3 depletion events were not considered. With the BrO + HCHO reaction (7) included (using the *Hansen et al.* [1999] rate coefficient), the simulation showed only a 17–11 ppt (34–16%) increase in HCHO compared with the halogen-free base run. This is reasonably consistent with the *Rudolph et al.* [1999] moderate O_3 destruction scenario above. Such small increases in HCHO through gas-phase halogen chemistry cannot explain the observed HCHO mixing ratios at Neumayer. A run omitting reaction (7) resulted in a doubling of the HCHO produced by halogen chemistry, showing that the BrO reaction is a significant sink for HCHO if the *Hansen et al.* [1999] rate coefficient is appropriate.

[70] Note that halogen production is a heterogeneous process. The effect of heterogeneous chemistry in general is largely neglected in most common photochemical models. If clouds can take up HCHO, this will lead to model calculations overestimating HCHO in the higher atmosphere during cloudy periods [*Fried et al.*, 2003a]. On the other hand, it is likely that ice particles in clouds will catalyze reactions that would not take place in the gas-phase, for example, the conversion of methanol to HCHO [*Jaeglé et al.*, 2000]. At present, we cannot include such processes in our model.

4.6. Model Runs With All Precursors

[71] After investigating the effects of different precursors on HCHO production, we combined all chemistry modules and investigated the joint effect. We set up the model for November, when 479 ppt HCHO were observed in the atmosphere. For reference, the constraints on the model were as follows: CH_4, 1697 ppb; CO, 61 ppb; O_3, 18 ppb; H_2O_2, 298 ppt; MHP, 191 ppt; NO_x, 5–10 ppt. On the basis of results in earlier sections, we chose the following values to represent plausible amounts of HCHO precursors in the atmosphere at Neumayer in November: DMS, 100 ppt; halogens: Cl, 5×10^3 molecules cm^{-3} and Br, 1.5×10^6 molecules cm^{-3}. We also considered two non-methane hydrocarbon (NMHC) scenarios: A: isoprene, 60 ppt; propene, 24 ppt (produced by isoprene oxidation); ethene, 45 ppt; and B: isoprene, 5 ppt; propene, 10 ppt; ethene, 25 ppt. Scenario B was suggested by recent measurements at Halley Bay, Antarctica (A. Lewis, personal communication, 2005).

[72] We initially ran the model for scenario A with all precursors included, but with the BrO + HCHO reaction (section 4.5) omitted. The HCHO flux from the snow was increased until the observed HCHO value of 479 ppt was obtained. The required HCHO flux was 1.9×10^{13} molecules m^{-2} s^{-1}. We then sequentially omitted each precursor in turn, restoring the previously omitted precursor to minimize nonlinear effects. This allowed us to estimate the approximate HCHO contribution of each precursor. The results (including CH_4) were as follows, given as a percentage of 479 ppt of HCHO: CH_4 8.6%; isoprene (including 24 ppt of propene produced by isoprene oxidation) 21.8%; ethene 0.7%; DMS 0.2%; halogens 6.0%; snow flux 62.7%. The total contribution of the individual precursors added linearly was 99.9%, showing that essentially no nonlinear effect was present. Thus, about 37% of the observed HCHO in November at Neumayer could be attributed to gas-phase precursors in the atmosphere if the NMHC values used were reasonable. Note that, with H_2O_2 and MHP constrained to observed values and with all other precursors present, CH_4 generated only about 9% of the observed HCHO. An isoprene mixing ratio of 60 ppt produced a relatively large 22% of the required HCHO.

[73] We carried out the same simulation sequence with NMHC scenario B. In this case, the required HCHO flux was 2.5×10^{13} m^{-2} s^{-1}. The results (including CH_4) were as follows, given as a percentage of 479 ppt of HCHO: CH_4, 14.8%; isoprene, 3.1%; propene, 0.7%; ethene, 0.6%; DMS, 0.7%; halogens, 2.5%; snow flux, 77.8%.

[74] These simulations suggest that about 60–80% of the HCHO measured at Neumayer in November is derived from direct snow emissions through a HCHO flux of $1.9–2.5 \times 10^{13}$ m^{-2} s^{-1}. This is significantly larger than fluxes so far observed at Summit, Greenland, or South Pole, Antarctica. To make our inferred flux values compatible with the Summit or South Pole measurements, a mean boundary layer height of the order of 5–10 m would be required throughout November. This seems unlikely. In any case, HCHO flux measurements are required at Neumayer to test these simulation results.

[75] We repeated the simulation sequence for scenario A including the BrO + HCHO reaction discussed in section 4.5, using the rate coefficient of 1.5×10^{-14} cm^3 $molecule^{-1}$ s^{-1} proposed by *Hansen et al.* [1999]. This produced a large perturbation to the system. The initial run with all precursors now required a HCHO flux of 2.5×10^{13} molecules m^{-2} s^{-1}, and halogens were found to contribute a HCHO decrease of 15% rather than an increase as in the set of simulations without the BrO + HCHO reaction. The total contribution of all precursors added linearly was 83%, showing that a large nonlinearity was present. This profound effect of a single reaction suggests that a much smaller rate coefficient for the BrO + HCHO reaction would be appropriate, as proposed by *Orlando et al.* [2000]. When we ran the simulations with a rate coefficient of 2×10^{-15} cm^3 $molecule^{-1}$ s^{-1}, consistent with the results of *Orlando et al.* [2000], the HCHO production percentages were only slightly different from the values quoted for scenario A when the BrO + HCHO reaction was omitted.

5. Summary and Conclusions

[76] We initially applied a simple gas phase photochemical box model to the full seasonal cycle of atmospheric measurements at Neumayer Station, Antarctica, described by *Riedel et al.* [1999, 2000]. This model included no emission or deposition of HCHO, H_2O_2, or MHP. The results showed large underestimation of HCHO and overestimation of H_2O_2 and MHP compared with the measurements, particularly in Antarctic spring (during the time of stratospheric ozone depletion) and summer.

[77] We then included emission and deposition fluxes of HCHO, H_2O_2, and MHP in the model, and adjusted these fluxes simultaneously to give simulated monthly mean mixing ratios of these species that matched the Neumayer measurements. The results showed that deposition of both H_2O_2 and MHP was required throughout the year, except for midwinter when no significant deposition or emission was required. However, to match our HCHO observations,

we had to include net HCHO emission fluxes of up to 3.2 × 10^{13} molecules m^{-2} s^{-1}, this value being required in November when ozone depletion in Antarctica reaches a maximum. For comparison, a maximum HCHO flux of 4.2 × 10^{12} molecules m^{-2} s^{-1} was reported for Arctic measurements [*Jacobi et al.*, 2002].

[78] The net HCHO emission flux in the model was intentionally not linked to any particular mechanism, as we wished to determine the total emission required from any source or combination of sources, both direct and indirect. We then considered the likely contributions of a variety of plausible direct and indirect sources, namely, snow surface emission, DMS, isoprene, ethene and propene, and halogen chemistry. However, none of the gas phase sources, even in combination, could reasonably approach the HCHO input required to match the observations, particularly in November. We found that at most 20–40% of the HCHO required in November could arise from gas phase precursors, including methane. The 40% value required 60 ppt of isoprene, which is not very likely near the Antarctic coast.

[79] We consider that a large flux of HCHO from the snow surface is required to explain the elevated HCHO concentrations observed at Neumayer Station in November. The remaining 60–80% of the observed HCHO in the boundary layer after gas phase precursors are excluded would require a HCHO flux from the snow of 1.9–2.5 × 10^{13} molecules m^{-2} s^{-1} with a mean boundary layer height of 41.5 m.

[80] A mean boundary layer height of 5–10 m throughout November would be required to reduce this flux to a value comparable with those measured at Summit, Greenland, and South Pole, Antarctica. Further measurements need to be made at Neumayer. Future campaigns should include measurements of HCHO fluxes from the snow, atmospheric hydrocarbon mixing ratios (in particular isoprene, ethene, and propene), J values, boundary layer height, and measurements of nitrous oxides (NO and NO_2) in order to test the simulation results described in this paper.

[81] **Acknowledgments.** This work was funded by the Royal Society of New Zealand Marsden Research Fund (contract NIW201) and the New Zealand Foundation for Research, Science and Technology (contract C01X0204). Part of the work was presented at the Young Scientists' Global Change Conference, organized by START and hosted by the Third World Academy of Sciences/CTP in Trieste, Italy. We thank Sasha Madronich and Sylvia Nichol for assistance with running the TUV radiative transfer model; Jill Cainey for modifying and running the DMS module of the NIWA model; and Daniel Jacob for his help with initiating the first model calculations using the Harvard model.

References

Allan, W., D. C. Lowe, and J. M. Cainey (2001), Active chlorine in the remote marine boundary layer: Modeling anomalous measurements of δ13C in methane, *Geophys. Res. Lett.*, *28*(17), 3239–3242.

Atkinson, R., D. L. Baulch, R. A. Cox, J. N. Crowley, R. F. Hampson, J. A. Kerr, M. J. Rossi, and J. Troe (2002), Summary of evaluated kinetic and photochemical data for atmospheric chemistry, IUPAC Subcomm. on Gas Kinet. Data Eval. for Atmos. Chem., Chem. Kinet. Data Cent., Natl. Inst. of Stand. and Technol., Gaithersburg, Md. (Available at http://www.iupac-kinetic.ch.cam.ac.uk)

Ayers, G. P., S. T. Bently, J. P. Ivey, and B. W. Forgan (1995), Dimethylsulfide in marine air at Cape Grim, 41°S, *J. Geophys. Res.*, *100*, 21,013–21,021.

Ayers, G. P., R. W. Gillett, H. Granek, C. de Servers, and R. A. Cox (1997), Formaldehyde production in clean marine air, *Geophys. Res. Lett.*, *24*(4), 401–404.

Berresheim, H., J. W. Huey, R. P. Thorn, F. L. Eisele, D. J. Tanner, and A. Jefferson (1998), Measurements of dimethyl sulfide, dimethyl sulfoxide, dimethyl sulfone, and aerosol ions at Palmer Station, Antarctica, *J. Geophys. Res.*, *103*(D1), 1629–1638.

Blake, D. R., T.-Y. Chen, T. W. Smith, C. J.-L. Wang, O. W. Wingenter, N. J. Blake, and F. S. Rowland (1996), Three-dimensional distribution of non-methane hydrocarbons and halocarbons over the northwestern Pacific during the 1991 Pacific Exploratory Mission (PEM-West A), *J. Geophys. Res.*, *101*(D1), 1763–1778.

Bottenheim, J. W., H. Boudries, P. C. Brickell, and E. Atlas (2002), Alkenes in the Arctic boundary layer at Alert, Nunavut, Canada, *Atmos. Environ.*, *36*, 2585–2594.

Boudries, H., and J. W. Bottenheim (2000), Cl and Br atom concentration during a surface boundary layer ozone depletion event in the Canadian High Arctic, *Geophys. Res. Lett.*, *27*(4), 517–520.

Broadgate, W., P. S. Liss, and S. A. Penkett (1997), Seasonal emissions of isoprene and other reactive hydrocarbon gases from the ocean, *Geophys. Res. Lett.*, *24*(21), 2675–2678.

Carter, W., and R. Atkinson (1996), Development and evaluation of a detailed mechanism for the atmospheric reactions of isoprene and NO_x, *Int. J. Chem. Kinet.*, *28*, 497–530.

Chu, L., and C. Anastasio (2003), Quantum yields of hydroxyl radical and nitrogen dioxide from the photolysis of nitrate on ice, *J. Phys. Chem. A*, *107*, 9594–9602.

Cox, R. A. (1999), Ozone and peroxy radical budgets in the marine boundary layer: Modeling the effect of NO_x, *J. Geophys. Res.*, *104*, 8047–8056.

Curran, M. A. J., and G. B. Jones (2000), Dimethyl sulfide in the Southern Ocean: Seasonality and flux, *J. Geophys. Res.*, *105*(D16), 20,451–20,459.

Dassau, T. M., et al. (2002), Investigation of the role of snowpack on atmospheric formaldehyde chemistry at Summit, Greenland, *J. Geophys. Res.*, *107*(D19), 4394, doi:10.1029/2002JD002182.

Davis, D., et al. (2001), Unexpected high levels of NO observed at South Pole, *Geophys. Res. Lett.*, *28*(19), 3625–3628.

de Bruyn, W. J., M. Harvey, J. M. Cainey, and E. S. Saltzman (2002), DMS and SO_2 at Baring Head, New Zealand: Implications for the yield of SO_2 from DMS, *J. Atmos. Chem.*, *41*, 189–209.

de Serves, C. (1994), Gas phase formaldehyde and peroxide measurements in the Arctic atmosphere, *J. Geophys. Res.*, *99*, 25,391–25,398.

Dibb, J. E., and S. I. Whitlow (1996), Recent climate anomalies and their impact on snow chemistry at South Pole, 1987–1994, *Geophys. Res. Lett.*, *23*(10), 1115–1118.

Dibb, J. E., M. Arsenault, M. C. Peterson, and R. E. Honrath (2002), Fast nitrogen oxide photochemistry in Summit, Greenland, snow, *Atmos. Environ.*, *36*(15–16), 2501–2511.

Dominé, F., and P. B. Shepson (2002), Air-snow interactions and atmospheric chemistry, *Science*, *297*, 1506–1510.

Dong, S., and P. K. Dasgupta (1987), Fast flow injection analysis of formaldehyde in atmospheric water, *Environ. Sci. Technol.*, *21*, 581–588.

Fried, A., et al. (2003a), Airborne tunable diode laser measurements of formaldehyde during TRACE-P: Distributions and box-model comparisons, *J. Geophys. Res.*, *108*(D20), 8798, doi:10.1029/2003JD003451.

Fried, A., et al. (2003b), Tunable diode laser measurements of formaldehyde during the TOPSE 2000 study: Distributions, trends, and model comparisons, *J. Geophys. Res.*, *108*(D4), 8365, doi:10.1029/2002JD002208.

Frost, G. J., et al. (2002), Comparisons of box model calculations and measurements of formaldehyde from the 1997 North Atlantic Regional Experiment, *J. Geophys. Res.*, *107*(D8), 4060, doi:10.1029/2001JD000896.

Grannas, A. M., et al. (2002), A study of photochemical processes affecting carbonyl compounds in the Arctic atmospheric boundary layer, *Atmos. Environ.*, *36*, 2733–2742.

Grannas, A. M., P. B. Shepson, and T. R. Filley (2004), Photochemistry and nature of organic matter in Arctic and Antarctic snow, *Global Biogeochem. Cycles*, *18*, GB1006, doi:10.1029/2003GB002133.

Grenfell, T. C., S. G. Warren, and P. C. Mullen (1994), Reflection of solar radiation by the Antarctic snow surface at ultraviolet, visible, and near-infrared wavelengths, *J. Geophys. Res.*, *99*, 18,669–18,684.

Handorf, D., T. Foken, and C. Kottmeier (1999), The stable atmospheric boundary layer over an Antarctic ice sheet, *Boundary Layer Meteorol.*, *91*, 165–189.

Hansen, J. C., Y. Li, J. S. Francisco, and Z. Li (1999), On the mechanism of the BrO + CH_2O reaction, *J. Phys. Chem.*, *103*, 8543–8546.

Hauglustaine, D. A., C. Granier, G. P. Brasseur, and G. Megie (1994), The importance of atmospheric chemistry in the calculation of radiative forcing on the climate system, *J. Geophys. Res.*, *99*, 1173–1186.

Honrath, R. E., M. C. Peterson, S. Guo, J. E. Dibb, P. B. Shepson, and B. Campbell (1999), Evidence of NO_x production within or upon ice particles in the Greenland snowpack, *Geophys. Res. Lett.*, *26*(6), 696–698.

Hopkins, J. R., I. D. Jones, A. C. Lewis, J. B. McQuaid, and P. W. Seakin (2002), Non-methane hydrocarbons in the Arctic boundary layer, *Atmos. Environ.*, *36*, 3217–3229.

Hough, A. M. (1991), Development of a two-dimensional global tropospheric model: Model chemistry, *J. Geophys. Res.*, *96*, 7325–7362.

Hutterli, M. A., R. Röthlisberger, and R. C. Bales (1999), Atmosphere-to-snow-to-firn transfer studies of HCHO at Summit, Greenland, *Geophys. Res. Lett.*, *26*(12), 1691–1694.

Hutterli, M. A., R. C. Bales, J. R. McConnell, and R. W. Stewart (2002), HCHO in Antarctic snow: Preservation in ice cores and air-snow exchange, *Geophys. Res. Lett.*, *29*(8), 1235, doi:10.1029/2001GL014256.

Hynes, A. J., P. H. Wine, and D. H. Semmes (1986), Kinetics and mechanism of OH reactions with organic sulphides, *J. Phys. Chem.*, *90*, 4148–4156.

Jacobi, H.-W., M. M. Frey, M. A. Hutterli, R. C. Bales, O. Schrems, N. J. Cullen, K. Steffen, and C. Koehler (2002), Measurements of hydrogen peroxide and formaldehyde exchange between the atmosphere and surface snow at Summit, *Atmos. Environ.*, *36*, 2619–2628.

Jaeglé, L., et al. (2000), Photochemistry of HO_x in the upper troposphere at northern midlatitudes, *J. Geophys. Res.*, *105*, 3877–3892.

Jobson, B. T., H. Niki, Y. Yokouchi, J. Bottenheim, F. Hopper, and R. Leaitch (1994), Measurements of C_2-C_6 hydrocarbons during the Polar Sunrise Experiment: Evidence for Cl atom and Br atom chemistry, *J. Geophys. Res.*, *99*, 25,355–25,368.

Jones, A. E., R. Weller, A. Minikin, E. W. Wolff, W. T. Sturges, H. P. McIntyre, S. R. Leonard, O. Schrems, and S. Bauguitte (1999), Oxidized nitrogen chemistry and speciation in the Antarctic troposphere, *J. Geophys. Res.*, *104*, 21,355–21,366.

Jones, A. E., R. Weller, E. W. Wolff, and H.-W. Jacobi (2000), Speciation and rate of photochemical NO and NO_2 production in Antarctic snow, *Geophys. Res. Lett.*, *27*(3), 345–348.

Jourdain, B., and M. Legrand (2001), Seasonal variations of atmospheric dimethylsulfide, dimethylsulfoxide, sulfur dioxide, methane–sulfonate, and non-sea-salt sulfate aerosols at Dumont d'Urville (coastal Antarctica) December 1998 to July 1999), *J. Geophys. Res.*, *106*(D13), 14,391–14,408.

Junkermann, W., and W. R. Stockwell (1999), On the budget of photooxidants in the marine boundary layer of the tropical South Atlantic, *J. Geophys. Res.*, *104*(D7), 8039–8046.

Kleefeld, C. (1998), Investigations of the seasonality of atmospheric dimethyl sulfide in the Arctic and Antarctica, *Rep. Polar Mar. Res.*, *257*, 1–168.

König-Langlo, G., J. C. King, and P. Pettré (1998), Climatology of the three coastal Antarctic stations Dumont d'Urville, Neumayer, and Halley, *J. Geophys. Res.*, *103*, 10,935–10,946.

Lazrus, A. L., G. L. Kok, S. N. Gitlin, and J. A. Lind (1985), Automated fluorometric method for hydrogen peroxide in atmospheric precipitation, *Anal. Chem.*, *57*, 917–922.

Lee, Y.-N., et al. (1998), Atmospheric chemistry and distribution of formaldehyde and several multioxygenated carbonyl compounds during the 1995 Nashville/Middle Tennessee Ozone Study, *J. Geophys. Res.*, *103*(D17), 22,449–22,462.

Lehrer, E., G. Hönninger, and U. Platt (2004), The mechanism of halogen liberation in the polar troposphere, *Atmos. Chem. Phys. Discuss.*, *4*, 3607–3652.

Lewis, A. C., L. J. Carpenter, and M. J. Pilling (2001), Nonmethane hydrocarbons in Southern Ocean boundary layer air, *J. Geophys. Res.*, *106*, 4987–4994.

Liss, P. S., and L. Merlivat (1986), Air-sea exchange rates: Introduction and synthesis, in *The Role of Air-Sea Exchange in Geochemical Cycling*, edited by P. Buat-Menard, pp. 113–127, Springer, New York.

Lowe, D. C., and U. Schmidt (1983), Formaldehyde (HCHO) measurements in the nonurban atmosphere, *J. Geophys. Res.*, *88*, 10,844–10,858.

Madronich, S., and S. Flocke (1998), The role of solar radiation in atmospheric chemistry, in *Handbook of Environmental Chemistry*, edited by P. Boule, pp. 1–26, Springer, New York.

Marti, J., and K. Mauersberger (1993), A survey and new measurements of ice vapor pressure at temperatures between 170 and 250 K, *Geophys. Res. Lett.*, *20*, 363–366.

Michalowski, B. A., J. S. Francisco, S.-M. Li, L. A. Barrie, J. W. Bottenheim, and P. B. Shepson (2000), A computer model study of multiphase chemistry in the Arctic boundary layer during polar sunrise, *J. Geophys. Res.*, *105*(D12), 15,131–15,145.

Nichol, S. E., G. Pfister, G. E. Bodeker, R. L. McKenzie, and S. W. Wood (2003), Moderation of cloud reduction of UV in the Antarctic due to high surface albedo, *J. Appl. Meteorol.*, *42*, 1174–1183.

Niki, H., P. D. Maker, C. M. Savage, and L. P. Breitenbach (1978), Mechanism for hydroxyl radical initiated oxidation of olefin-nitric oxide mixtures in parts per million concentrations, *J. Phys. Chem.*, *82*, 135–137.

Niki, H., P. D. Maker, C. M. Savage, and L. P. Breitenbach (1981), An FTIR study of mechanisms for the HO radical initiated oxidation of C_2H_4 in the presence of NO: Detection of glycolaldehyde, *Chem. Phys. Lett.*, *80*, 499–503.

Novelli, P. C., K. A. Masarie, P. P. Tans, and P. M. Lang (1994), Recent changes in atmospheric carbon monoxide, *Science*, *263*, 1587–1590.

Orlando, J. J., B. Ramacher, and G. S. Tyndall (2000), Upper limits for the rate coefficients for reactions of BrO with formaldehyde and HBr, *Geophys. Res. Lett.*, *27*, 2633–2636.

O'Sullivan, D. W., B. G. Heikes, M. Lee, W. Chang, G. L. Gregory, D. R. Blake, and G. W. Sachse (1999), Distribution of hydrogen peroxide and methylhydroperoxide over the Pacific and South Atlantic Oceans, *J. Geophys. Res.*, *104*, 5635–5646.

Palmer, P. I., D. J. Jacob, A. M. Fiore, R. V. Martin, K. Chance, and T. P. Kurosu (2003), Mapping isoprene emissions over North America using formaldehyde column observations from space, *J. Geophys. Res.*, *108*(D6), 4180, doi:10.1029/2002JD002153.

Platt, U. (2002), The impact of halogen chemistry on the oxidation capacity of the troposphere, in *Global Atmospheric Change and Its Impact on Regional Air Quality*, *NATO Sci. Ser.*, vol. 4, *Earth and Environmental Sciences*, vol. 16, edited by I. Barnes, Springer, New York.

Ridley, B. A., et al. (2003), Ozone depletion events observed in high latitude surface layer during the Tropospheric Ozone Production about the Spring Equinox (TOPSE) aircraft program, *J. Geophys. Res.*, *108*(D4), 8356, doi:10.1029/2001JD001507.

Riedel, K. (2001), Investigation of the photooxidants hydrogen peroxide, methylhydroperoxide and formaldehyde in the troposphere of Antarctica, *Rep. Polar Mar. Res.*, *394*, 1–153.

Riedel, K., R. Weller, and O. Schrems (1999), Variability of formaldehyde in the Antarctic troposphere, *Phys. Chem. Chem. Phys.*, *1*, 5523–5527.

Riedel, K., R. Weller, O. Schrems, and G. König-Langlo (2000), Variability of tropospheric hydroperoxides at a coastal surface site in Antarctica, *Atmos. Environ.*, *34*, 5225–5234.

Riemer, D. D., P. J. Milne, R. G. Zika, and W. H. Pos (2000), Photoproduction of nonmethane hydrocarbons (NMHCs) in seawater, *Mar. Chem.*, *71*, 177–198.

Rudolph, J., A. Khedim, and D. Wagenbach (1989), The seasonal variation of light nonmethane hydrocarbons in the Antarctic troposphere, *J. Geophys. Res.*, *94*, 13,039–13,044.

Rudolph, J., B. R. Fu, A. Thompson, K. Anlauf, and J. Bottenheim (1999), Halogen atom concentrations in the Arctic troposphere derived from hydrocarbon measurements: Impact on the budget of formaldehyde, *Geophys. Res. Lett.*, *26*(19), 2941–2944.

Sander, S. P., D. M. Golden, M. J. Kurylo, G. K. Moortgat, A. R. Ravishankara, C. E. Kolb, M. J. Molina, and B. J. Finlayson-Pitts (2003), Chemical kinetics and photochemical data for use in atmospheric studies, Evaluation 14, *JPL Publ.*, *02-25*.

Schultz, M. G., et al. (1999), On the origin of tropospheric ozone and NO_x over the tropical South Pacific, *J. Geophys. Res.*, *104*, 5829–5843.

Seinfeld, J. H., and S. N. Pandis (1998), Tropospheric chemistry of halogen compounds, in *Atmospheric Chemistry and Physics: From Air Pollution to Climate Change*, John Wiley, Hoboken, N. J.

Shaw, S. L. (2001), The production of non-methane hydrocarbons by marine plankton, Ph.D. thesis, Cent. for Global Change Sci., Mass. Inst. of Technol., Cambridge. (Available at http://web.mit.edu/cgcs/www/MIT_CGCS_Rpt66.pdf)

Singh, H. B., et al. (2000), Distribution and fate of selected oxygenated organic species in the troposphere and lower stratosphere over the Atlantic, *J. Geophys. Res.*, *105*(D3), 3795–3805.

Spicer, C. W., E. G. Chapman, B. J. Finlayson-Pitts, R. A. Plastrige, J. M. Hubbe, J. D. Fast, and C. M. Berkowitz (1998), Unexpected high concentrations of molecular chlorine in coastal air, *Nature*, *394*, 353–356.

Sprengnether, M., K. L. Demerjian, N. M. Donahue, and J. G. Anderson (2002), Product analysis of the OH oxidation of isoprene and 1,3-butadiene in the presence of NO, *J. Geophys. Res.*, *107*(D15), 4268, doi:10.1029/2001JD000716.

Sumner, A. L., and P. B. Shepson (1999), Snowpack production of formaldehyde and its effect on the Arctic troposphere, *Nature*, *398*, 230–233.

Sumner, A. L., et al. (2002), Atmospheric chemistry of formaldehyde in the Arctic troposphere at polar sunrise, and the influence of the snowpack, *Atmos. Environ.*, *36*, 2553–2562.

Swanson, A. L., N. J. Blake, J. E. Dibb, M. R. Albert, D. R. Blake, and F. S. Rowland (2002), Photochemically induced production of CH_3Br, CH_3I, C_2H_5I, ethene, and propene within surface snow at Summit, Greenland, *Atmos. Environ.*, *36*, 2671–2682.

Urbanski, S. P., R. E. Stickel, Z. Zhao, and P. Wine (1997), Mechanistic and kinetic study of formaldehyde production in the atmospheric oxidation of dimethyl sulfide, *J. Chem. Soc., Faraday Trans.*, *93*(16), 2813–2819.

Wagner, V., R. von Glasow, H. Fischer, and P. J. Crutzen (2002), Are CH_2O measurements in the marine boundary layer suitable for testing the current understanding of CH_4 photooxidation?: A model study, *J. Geophys. Res.*, *107*(D3), 4029, doi:10.1029/2001JD000722.

Weller, R., O. Schrems, A. Boddenberg, S. Gäb, and M. Gautrois (2000), Meridional distribution of hydroperoxides and formaldehyde in the marine boundary layer of the Atlantic (48°N–35°S) measured during the ALBATROSS campaign, *J. Geophys. Res.*, *105*(D11), 14,401–14,412.

Weller, R., A. E. Jones, A. Wille, H.-W. Jacobi, H. P. McIntyre, W. T. Sturges, M. Huke, and D. Wagenbach (2002), Seasonality of reactive nitrogen oxides (NO_y) at Neumayer Station, Antarctica, *J. Geophys. Res.*, *107*(D23), 4673, doi:10.1029/2002JD002495.

Wert, B. P., et al. (2003), Signatures of terminal alkene oxidation in airborne formaldehyde measurements during the Texas Air Quality Study (TexAQS) 2000, *J. Geophys. Res.*, *108*(D3), 4104, doi:10.1029/2002JD002502.

Yin, F., D. Grosjean, and J. H. Seinfeld (1990), Photooxidation of dimethyl sulfide and dimethyl disulfide. I: Mechanism development, *J. Atmos. Chem.*, *11*, 309–364.

Yokouchi, Y., H.-J. Li, and T. Machida (1999), Isoprene in the marine boundary layer (Southeast Asian Sea, eastern Indian Ocean, and Southern Ocean): Comparison with dimethyl sulfide and bromoform, *J. Geophys. Res.*, *104*(D7), 8067–8076.

W. Allan and K. Riedel, National Institute of Water and Atmospheric Research, Private Bag 14-901, Wellington, New Zealand. (k.riedel@niwa.co.nz)

O. Schrems and R. Weller, Alfred Wegener Institute for Polar and Marine Research, Am Handelshafen 12, 27570 Bremerhaven, Germany.